Sensors and Materials, Vol. 38, No. 5 (2026) 2653–2660
MYU Tokyo

S & M 4460

Planar Marchand Balun with Double-layer Coupled Lines on FR4 Substrate

Ja-Hao Chen* and Cheng-Hsuan Hsieh

Department of Communications Engineering, Feng Chia University,
No. 100, Wenhwa Rd., Xitun Dist., Taichung 407102, Taiwan (R.O.C.)

(Received December 19, 2025; accepted March 24, 2026)

Keywords: Marchand balun, double-layer coupled line, isolation circuit

A planar Marchand balun with double-layer coupled lines on an FR4substrate is proposed. The double-layer coupled-line structure mitigates the low-coupling issue associated with the substrate's high dissipation factor, enhances the coupling coefficient of the coupled lines, and consequently improves the balun performance. An isolation circuit is employed to provide isolation and impedance matching between the balanced ports, facilitating circuit and system integration. The overall circuit is compact, occupying an area of 0.264 × 0.517 λ_g^2. Measurement results show that, within the 2–3 GHz band, the proposed Marchand balun achieves a return loss lower than 10 dB at both the unbalanced and balanced ports, an insertion loss of approximately 3.5 dB, and isolation between the balanced ports exceeding 15 dB. The fractional bandwidth is 60%. The amplitude and phase imbalances are less than 0.32 dB and 0.8°, respectively. The proposed balun offers a compact size, low cost, and competitive performance on an FR4 substrate, making it suitable for modern wireless communication system applications.

1. Introduction

Modern wireless communication front-end modules often use balanced circuit architectures, such as mixers, low-noise amplifiers, and power amplifiers, to enhance overall performance. When interfacing these modules with antennas, a microwave balun is required to convert balanced signals into unbalanced signals, with the Marchand balun being widely used. Originally proposed by Marchand in 1944,[1] it remains a topic of active research.[2–5] The conventional Marchand balun consists of two pairs of quarter-wavelength coupled lines with open- and short-circuited terminations, as illustrated in Fig. 1, and its S-parameter model under lossless conditions is given as follows.

*Corresponding author: e-mail: chiahaoc@fcu.edu.tw
https://doi.org/10.18494/SAM6129

ISSN 0914-4935

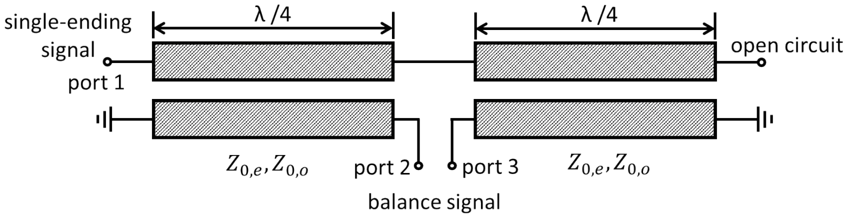

Fig. 1. Circuit configuration of a conventional Marchand balun.

$$\begin{bmatrix} S_{11} & S_{12} & S_{13} \\ S_{21} & S_{22} & S_{23} \\ S_{31} & S_{32} & S_{33} \end{bmatrix} = \begin{bmatrix} \dfrac{1-3c^2}{1+c^2} & j\dfrac{2c\sqrt{1-c^2}}{1+c^2} & -j\dfrac{2c\sqrt{1-c^2}}{1+c^2} \\ j\dfrac{2c\sqrt{1-c^2}}{1+c^2} & \dfrac{1-c^2}{1+c^2} & \dfrac{2c^2}{1+c^2} \\ -j\dfrac{2c\sqrt{1-c^2}}{1+c^2} & \dfrac{2c^2}{1+c^2} & \dfrac{1-c^2}{1+c^2} \end{bmatrix} \tag{1}$$

Here, c denotes the coupling coefficient of the coupled lines. When $c = \sqrt{1/3}$ (equivalently, $c = -4.77$ dB), the unbalanced port exhibits perfect impedance matching, and the insertion losses at the balanced ports are both 3 dB. The reflection coefficients and isolation at the balanced ports are 6.02 dB, indicating that perfect impedance matching and complete isolation cannot be achieved simultaneously at the balanced ports. To overcome this limitation, various techniques have been proposed to enhance the coupling coefficient(6–8) and to improve balanced-port matching and isolation by employing capacitors,(9) resistors,(10) and isolation circuits.(7,11) Although these balun circuits demonstrate good performance, they are implemented on high-cost substrates with relatively low dissipation factors.

Several balun circuits implemented on FR4 substrates have been reported.(12,13) Kumari *et al.* designed a balun using a rat-race coupler incorporating an interdigital capacitor structure, which provides low insertion loss and high isolation at the balanced port.(12) However, its structure limits the circuit's fractional bandwidth (FBW) to 37.5%, inhibits impedance matching at the balanced ports, and results in relatively high amplitude and phase imbalances. Deb *et al.* integrated two complementary split-ring resonators into the ground plane of a conventional Marchand balun to reduce insertion loss.(13) Nevertheless, this approach also suffers from a narrow FBW (18.75%), a lack of balanced-port matching and isolation, and a relatively high phase imbalance.

In this work, a double-layer coupled-line structure replaces the conventional coupled line to enhance the coupling coefficient and reduce insertion loss. An isolation circuit is employed to provide impedance matching and isolation at the balanced ports. Measurement results demonstrate that the proposed Marchand balun achieves good performance in the 2–3 GHz band when implemented on a high-dissipation, low-cost FR4 substrate. The balun features low insertion loss, good impedance matching and isolation, compact size, an FBW of 60%, ease of design, and cost-effective implementation for modern wireless communication systems.

2. Design of Proposed Marchand Balun

As indicated by Eq. (1), the coupling coefficient is critical to the performance of a Marchand balun. In this work, we present an analysis for enhancing the coupling coefficient of coupled lines. The lumped-element model of a conventional microstrip coupled line under even- and odd-mode excitations is shown in Figs. 2(a) and 2(b), where L_s and L_m are the self- and mutual inductances, and C_s and C_m represent the ground and interline capacitances, respectively. The coupling coefficient c is expressed in terms of the even- and odd-mode impedances, $Z_{0,e}$ and $Z_{0,o}$, respectively, as

$$c = \frac{Z_{0,e} - Z_{0,o}}{Z_{0,e} + Z_{0,o}} = \frac{\Lambda}{2 + \Lambda + 2\sqrt{\Lambda + 1}}, \tag{2}$$

where

$$Z_{0,e} = \sqrt{\frac{L_s + L_m}{C_s}}, \text{ and } Z_{0,o} = \sqrt{\frac{L_s}{C_s + 2C_m}}, \tag{3}$$

and the dimensionless parameter Λ is expressed as

$$\Lambda = \frac{L_m}{L_s} + 2\frac{C_m}{C_s}\left(1 + \frac{L_m}{L_s}\right). \tag{4}$$

As presented in Eq. (2), the coupling coefficient c increases monotonically with Λ. Furthermore, Eq. (4) indicates that the coupling coefficient c can be increased by enlarging the ratios L_m / L_s and C_m / C_s, that is, by increasing the mutual inductance and capacitance of the coupled lines

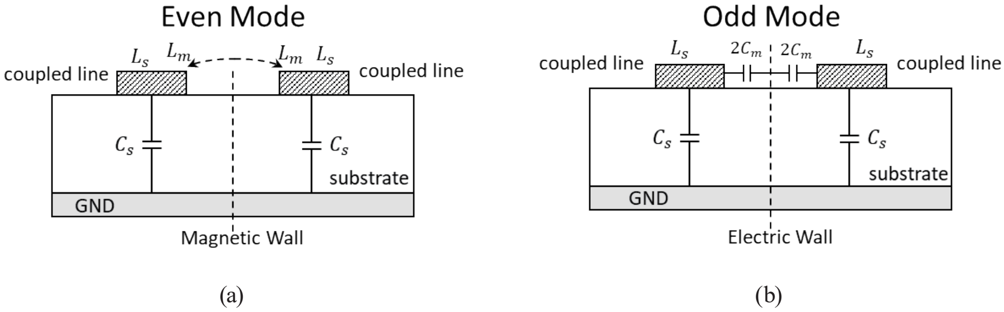

Fig. 2. Lumped-element model of conventional coupled line: (a) even mode and (b) odd mode.

while simultaneously reducing their self-inductance and self-capacitance. Motivated by this observation, a double-layer coupled-line structure is proposed to improve coupling.

Figure 3 shows the cross section of the double-layer coupled-line structure. The upper and lower microstrip lines are connected by vias, and the lower metal layer is isolated from ground by an etched trench. Figures 3(a) and 3(b) depict the equivalent lumped-element models under even- and odd-mode excitations, respectively. The resulting even- and odd-mode impedances, $Z_{0,e}$ and $Z_{0,o}$, respectively, and Λ for the double-layer structure are given as

$$Z_{0,e}^{'} = \sqrt{\frac{L_s^{'} + L_m^{'}}{C_s^{'}}},\ \text{and}\ Z_{0,o}^{'} = \sqrt{\frac{L_s^{'}}{C_s^{'} + 4C_m + 2C_{th}}}, \tag{5}$$

$$\Lambda = \frac{L_m^{'}}{L_s^{'}} + 2\left(\frac{2C_m + C_{th}}{C_s^{'}}\right)\left(1 + \frac{L_m^{'}}{L_s^{'}}\right), \tag{6}$$

where $L_s^{'}$ and $L_m^{'}$ are the self- and mutual inductances, respectively, $C_s^{'}$ is the ground capacitance, and C_{th} is the via-to-via capacitance. The double-layer coupled-line structure enlarges the coupling area and reduces the ground capacitance, resulting in $(2C_m + C_{th}) / C_s^{'} > C_m / C_s$. Electromagnetic simulations using an FR4 substrate of 0.8 mm thickness (ε_r = 4.4, tanδ = 0.02) show that the conventional quarter-wavelength coupled line with a spacing of 0.2 mm achieves a coupling coefficient of −10.12 dB, whereas the double-layer coupled line improves it to −4.78 dB at 2.4 GHz. A Marchand balun based on the double-layer coupled-line structure achieves simulated insertion losses of 3.27 and 3.32 dB. With a fixed substrate thickness, the coupling characteristics of dual-layer coupled lines can be enhanced by optimizing the line width, spacing, and via count. However, trade-offs between these parameters are necessary when considering impedance matching and fabrication constraints on the minimum spacing.

To ensure impedance matching and high isolation at the balanced ports for easy integration into the system, an isolation circuit[10] is introduced, as shown in Fig. 4. Z_{b2} and Z_{b3} are the output impedances (150 Ω), and Z_{m2} and Z_{m3} are the load impedances (50 Ω). The isolation transmission line is designed with a characteristic impedance of Z_{iso} = 100 Ω. The required impedance Z_1 is given by

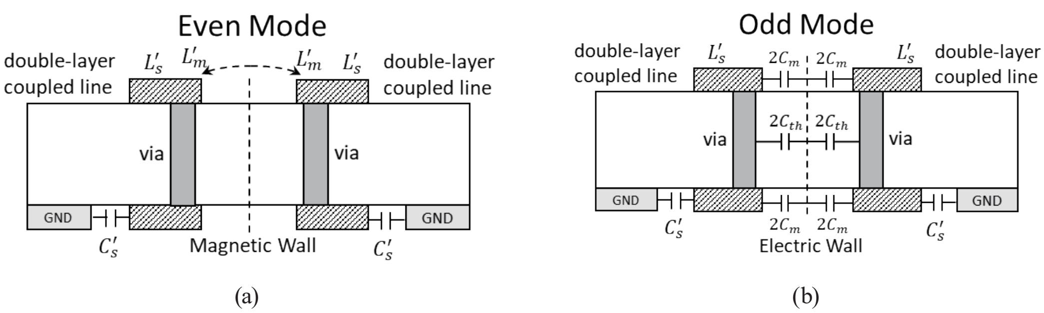

Fig. 3. Lumped-element model of double-layer coupled line: (a) even mode and (b) odd mode.

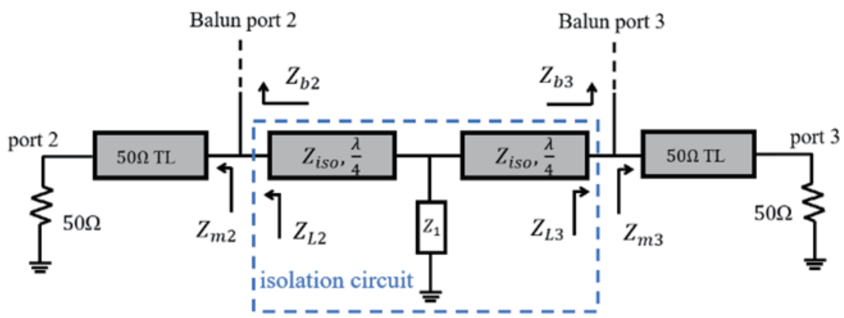

Fig. 4. (Color online) Isolation circuit used in the proposed balun.

$$Z_1 = \frac{Z_{iso}^2}{Z_{L2}} // \frac{Z_{iso}^2}{Z_{L3}}, \tag{7}$$

where $Z_{L2} = Z_{m2} // Z_{b2}$ and $Z_{L3} = Z_{m3} // Z_{b3}$, resulting in Z_1 = 133 Ω.

Figure 5 illustrates the three-dimensional structure of the proposed Marchand balun. The circuit incorporates two double-layer coupled lines and isolation circuits. Following electrical optimization using electromagnetic simulation software, the final balun dimensions shown in Fig. 6 are summarized in Table 1. It has a compact size of 18.06 × 35.35 mm^2 (i.e., 0.264 × 0.517 $\lambda_g{}^2$). The simulated S-parameters (dashed lines in Fig. 7) show return losses > 10 dB at the unbalanced port and at the balanced ports, isolation between the balanced ports exceeding 15 dB, and an insertion loss of approximately 3.5 dB across 2–3 GHz. Figure 8 shows the simulated amplitude and phase imbalances at the unbalanced port, both maintained below 0.2 dB and 0.34°, respectively, over the same frequency range.

3. Measured Results

Three Marchand balun circuits with double-layer coupled lines were implemented to verify the design. Process tolerances (e.g., PCB manufacturing, via connections, and SMA assembly) resulted in a measurement error of less than 5%. We have presented the representative result that reflects the median performance among the samples. Photographs of the fabricated circuit are shown in Fig. 7. The measured S-parameters, obtained using an Anritsu MS46122B vector network analyzer, show good agreement with the simulated results, as indicated by the solid lines in Fig. 8. Over the 2–3 GHz band, the measured return losses exceed 10 dB at both the balanced and unbalanced ports. At 2.4 GHz, the measured insertion losses are 3.44 and 3.65 dB, and the isolation reaches 19.2 dB.

Across the 2–3 GHz band, the measured amplitude imbalance varies between −0.23 and 0.36 dB, while the phase imbalance ranges from 179.26 to 180.3°, as shown in Fig. 9. A comparison of the performance characteristics of previously reported baluns and our proposed balun is shown in Table 2. The results show that the proposed balun can be fabricated on a low-cost, high-dissipation substrate while maintaining competitive performance.

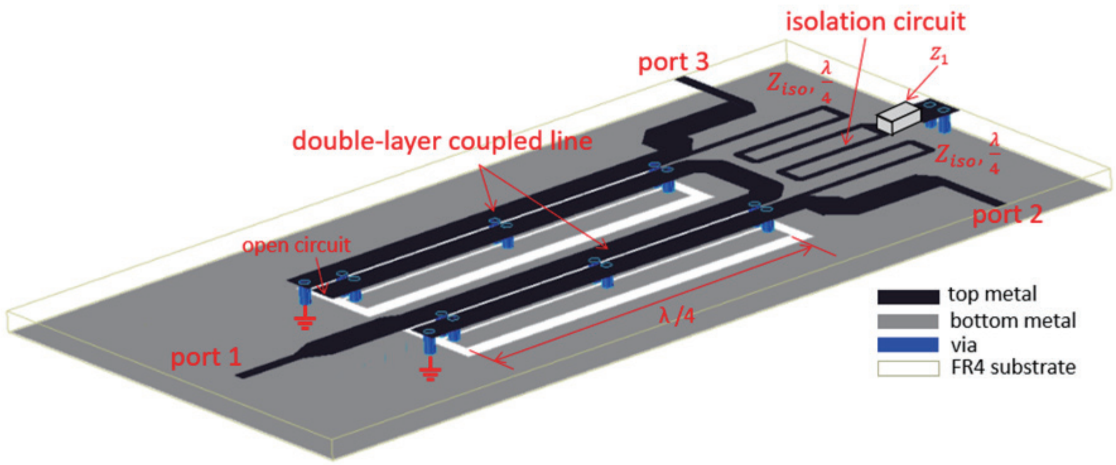

Fig. 5. (Color online) Three-dimensional perspective view of the proposed Marchand balun.

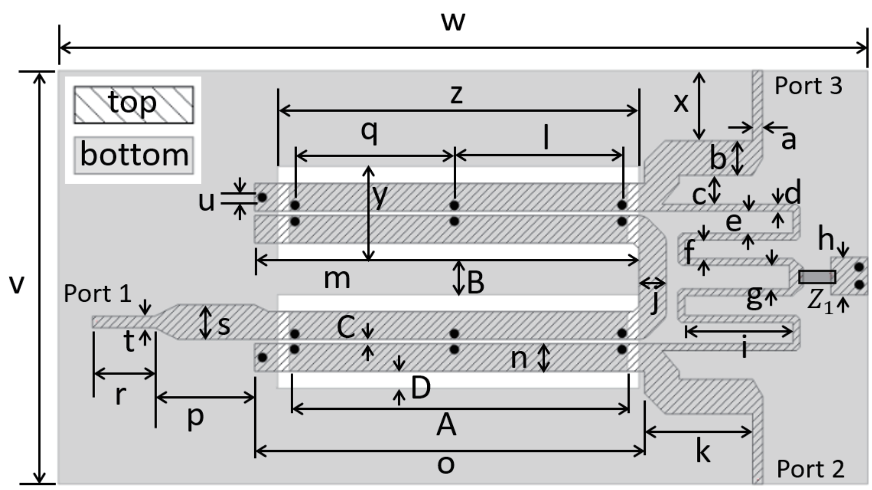

Fig. 6. Layout dimensions of the proposed Marchand balun. Values are given in Table 1.

Table 1
Geometric parameters of the proposed balun.

Dimension	Value (mm)	Dimension	Value (mm)	Dimension	Value (mm)
a	0.45	k	4.72	u	0.4
b	1.52	l	7.32	v	18.06
c	1.25	m	16.78	w	35.35
d	0.3	n	1.2	x	3.06
e	0.98	o	17.02	y	4.1
f	0.8	p	4.37	z	15.78
g	1.02	q	6.96	A	14.78
h	1.64	r	2.71	B	1.5
I	4.85	s	1.5	C	0.2
j	1.2	t	0.5	d	0.75

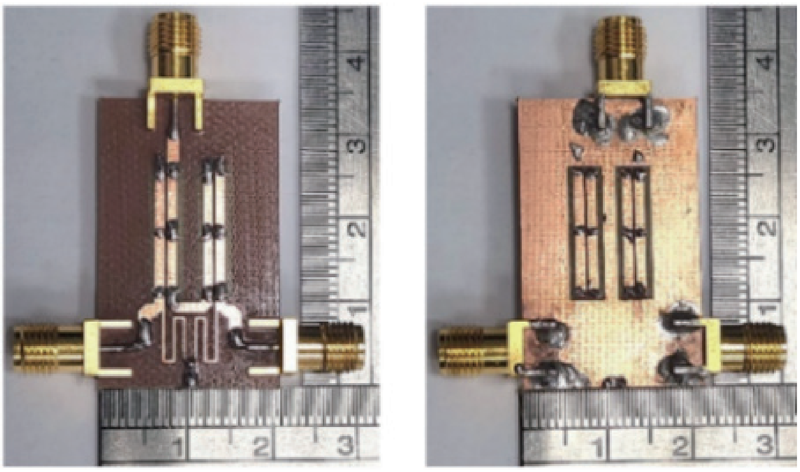

Fig. 7. (Color online) Photographs of the proposed balun: (a) top view and (b) bottom view.

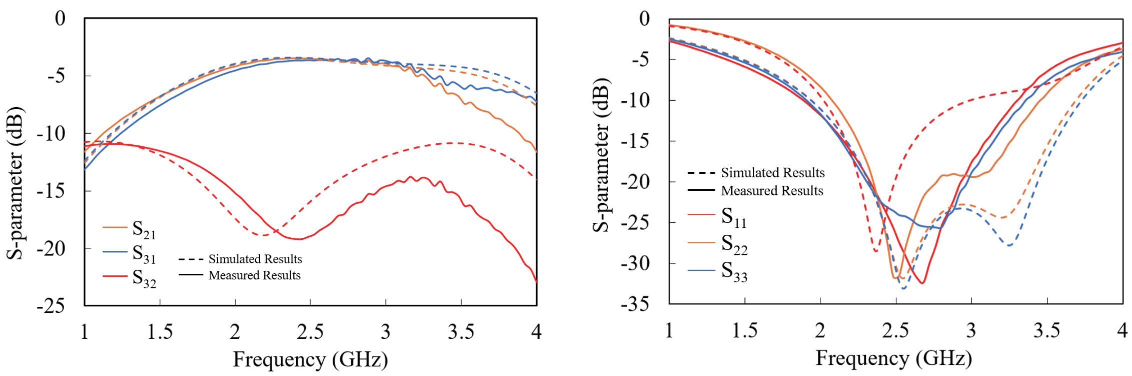

Fig. 8. (Color online) Simulated and measured S-parameters of the proposed balun. (a) Return losses: S_{11}, S_{22}, and S_{33}. (b) Insertion and isolation parameters: S_{21}, S_{31}, and S_{32}.

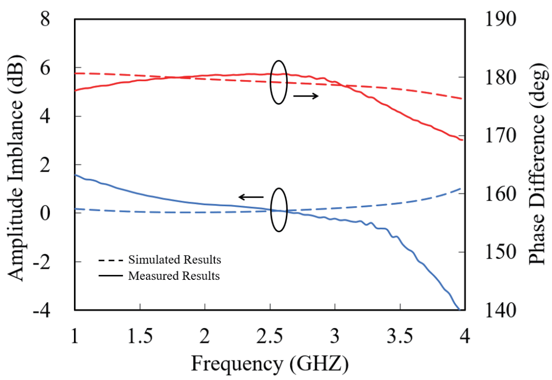

Fig. 9. (Color online) Simulated and measured amplitude imbalance and phase difference of the proposed balun.

Table 2
Performance characteristics of previously reported baluns and our proposed balun.

Study	Substrate	f_0 (GHz)	FBW (%)	Unbalanced port return loss (dB)	Balanced port return loss (dB)	Isolation (dB)	Insertion loss (dB)	Amplitude imbalance (dB)	Phase imbalance (degree)	Size (λ_g^2)
[6]	$\varepsilon_r = 2.55$	2.4	2	17	7.4	13.3	4.7, 4.3	0.4	4	0.3 × 0.3
[7]	RT 5870 $\varepsilon_r = 2.33$	0.7	40	34.2	30.2	35.8	3.28, 3.32	0.004	1.27	0.029 × 0.112
[8]/A	RT 6010 $\varepsilon_r = 10.2$	2.5	80	16	w/o matching	w/o isolation	3.82, 3.62	0.2	1	0.568 × 0.415
[8]/B	RT 6010 $\varepsilon_r = 10.2$	4.2	90	17	w/o matching	w/o isolation	3.49, 3.71	0.22	1	0.956 × 0.7
[10]	RT 6202 $\varepsilon_r = 2.94$	1.5	89.5	21.8	31.8	40	3.38, 2.94	0.44	1	0.44 × 0.44
[12]	FR4 $\varepsilon_r = 4.4$	2.4	37.5	20.99	w/o matching	23.14	2.9, 3.83	0.93	1.37	0.51 × 0.22
[13]	FR4 $\varepsilon_r = 4.4$	2.4	18.75	32.24	w/o matching	w/o isolation	3.75, 3.82	0.07	1.45	0.515 × 0.279
This work	FR4 $\varepsilon_r = 4.4$	2.4	60	22.55	22.5	19.2	3.44, 3.65	0.21	0.52	0.264 × 0.517

4. Conclusions

In this paper, a planar Marchand balun using double-layer coupled lines on an FR4 substrate presented. The double-layer coupled-line structure was analyzed and found to enhance the coupling coefficient of the coupled line, thereby improving the overall balun performance. An isolation circuit was incorporated to achieve proper impedance matching and high isolation at the balanced ports. Measured results demonstrated good impedance matching, high isolation, low insertion loss, a 60% FBW, and low amplitude and phase imbalances around 2.4 GHz. The proposed balun features a compact size, low cost, and competitive performance, making it suitable for modern wireless communication system applications.

References

1 N. Marchand: Electronics **17** (1944) 142.
2 J. Li, K, Liu, and T. Li: Microwave Opti. Technol. Lett. **64** (2022) 42.
3 S. Chakraborty, L. E. Milner, X. Zhu, A. Parker, and M. Heimlich: IEEE Trans. Circuits Syst. II: Express Briefs. **69** (2022) 4278.
4 J. Steele and D. Psychogiou: IEEE Trans. Microwave Theory Tech. **72** (2024) 5904.
5 E. M. Umar, M. Laabs, N. Neumann, and D. Plettemeier: 2025 16th German Microwave Conf. (GeMiC) 562.
6 J. M. Yan, H. Y. Zhou, and L. Z. Cao: IEEE Microwave Wireless Compon. Lett. **27** (2017) 1056.
7 H. R. Ahn and M. M. Tentzeris: IEEE Trans. Circuits and Syst. II: Express Briefs **67** (2020) 2299.
8 J. Li, K. Liu, and T. Li: Microwave Opt. Technol. Letter **64** (2022) 42.
9 K. S. Ang, Y. C. Leong, and C. H. Lee: IEEE Trans. Microwave Theory Tech. **51** (2003) 1009.
10 W. Chen, Y. Wu, and W. Wang: IEEE Trans. Circuits Syst. II: Express Briefs **67** (2020) 1884.
11 H. R. Ahn and T. Itoh: IEEE Trans. Microwave Theory Tech. **58** (2010) 3892.
12 A. Kumari, P. Bhowmik, and T. Moyra: AEU Int. J. Electron. Commun. **95** (2018) 155.
13 P. K. Deb, T. Moyra, and B. K. Bhattacharyya: IET Microwaves, Antennas Propag. **15** (2021) 788.